JOURNAL OF COMPUTATIONAL PHYSICS 46, 329–341 (1982)

A Stability-Enhancing Two-Step Method for Fluid Flow Calculations*

JOHN H. MAHAFFY

Safety-Code Development, Energy Division,
Los Alamos National Laboratory, Los Alamos, New Mexico 87545

Received May 12, 1981; revised February 17, 1982

An extension is presented of semi-implicit methods such as the implicit continuous Eulerian (ICE) technique for modeling fluid flow. This new approach eliminates the material Courant stability limit associated with semi-implicit methods at little additional computational cost.

I. INTRODUCTION

During the past decade, various semi-implicit finite-difference schemes such as the ICE method [1] have been used widely for solving problems in fluid flow. In many problems of interest, however, the stability limit on time-step size (less than the mesh size divided by the material velocity) associated with this class of methods is far smaller than is necessary for reasonable accuracy. In such cases the standard approach for cutting computational costs is to eliminate this material Courant limit with a fully implicit difference method; or, in multidimensional problems, employ an alternating direction implicit (ADI) scheme [2]. Here we present a less costly way to permit the use of larger time-step sizes.

The stability-enhancing two-step (SETS) method was designed to propagate information needed for stability with minimal implicit coupling between spatial nodes. Information about pressure wave propagation is provided with a basic step, which is simply a semi-implicit equation set. A stabilizing step is then added to provide the necessary flow of information about the density, energy, and momentum being transported across cell boundaries. Because the stabilizing step is separated from the basic step, this approach has the further advantage that existing semi-implicit codes can be converted to the SETS method with relative ease.

The first practical application of this method was in the field of nuclear reactor safety. A sample reactor calculation is presented in this paper to demonstrate the advantages of a reactor safery code based on SETS over one based on semi-implicit techniques.

* This work was performed under the auspices of the United States Nuclear Regulatory Commission.

0021-9991/82/060329-13$02.00/0

II. Basic Equations

To demonstrate the SETS method we shall consider a simplified model for one-dimensional single-phase flow in a straight pipe. The differential equations for this model are

$$\frac{\partial \rho}{\partial t} + \frac{\partial \rho V}{\partial x} = 0, \tag{1}$$

$$\frac{\partial \rho e}{\partial t} + \frac{\partial \rho e V}{\partial x} = -p \frac{\partial V}{\partial x}, \tag{2}$$

and

$$\frac{\partial V}{\partial t} + V \frac{\partial V}{\partial x} = -\frac{1}{\rho} \frac{\partial p}{\partial x} - KV|V|. \tag{3}$$

Here K is a wall friction coefficient that may be a function of velocity and fluid properties.

The spatial mesh used for the finite-difference equations is staggered, with thermodynamic properties evaluated at the cell centers and the velocity evaluated at the cell edges. To ensure stability and maintain consistency with differencing in existing reactor safety codes [3], flux terms at cell edges use donor cell averages of the form

$$\begin{aligned} \langle YV \rangle_{j+1/2} &= Y_j V_{j+1/2}, \qquad V_{j+1/2} \geqslant 0 \\ &= Y_{j+1} V_{j+1/2}, \qquad V_{j+1/2} < 0. \end{aligned} \tag{4}$$

Other forms of this average may maintain stability with higher-order spatial accuracy but they have not been studied carefully. With this notation the one-dimensional finite-difference divergence operator is

$$\nabla_j \cdot (YV) = (\langle YV \rangle_{j+1/2} - \langle YV \rangle_{j-1/2})/\Delta x_j, \tag{5}$$

and term $V \nabla V$ becomes

$$\begin{aligned} V_{j+1/2} \nabla_{j+1/2} V &= V_{j+1/2}(V_{j+1/2} - V_{j-1/2})/\Delta x_{j+1/2}, \qquad V_{j+1/2} \geqslant 0 \\ &= V_{j+1/2}(V_{j+3/2} - V_{j+1/2})/\Delta x_{j+1/2}, \qquad V_{j+1/2} < 0, \end{aligned} \tag{6}$$

where $\Delta x_{j+1/2} = 0.5\ (\Delta x_j + \Delta x_{j+1})$. This choice of $\Delta x_{j+1/2}$ for Eq. (6) rather than one obtained from a donor cell average was found necessary for more accurate calculation of pressure drops in pipes modeled with a nonuniform mesh.

For the flow model given by Eqs. (1)–(3), the combination of basic and stabilizer equation sets can be written in a number of ways without significantly affecting the results of calculations. For example, the stabilizer step may precede the basic step for all equations, or the basic step may be done before the stabilizer step. When the

SETS method is adapted to the two-fluid model for two-phase flow, it has been found that several orderings of the difference equations can cause growing oscillations due to feedback through interfacial friction terms. One ordering that is always stable begins with the stabilizer step for the equations of motion, is followed by a solution of the basic equation set for all equations, and ends with a stabilizer step for the mass and energy equations. For this ordering the SETS finite-difference equations for Eqs. (1)–(3) are:

Stabilizer Equation of Motion

$$(\tilde{V}^{n+1}_{j+1/2} - V^n_{j+1/2})/\Delta t + V^n_{j+1/2}\nabla_{j+1/2}\tilde{V}^{n+1} + \beta(\tilde{V}^{n+1}_{j+1/2} - V^n_{j+1/2})\nabla_{j+1/2}\tilde{V}^n + \frac{1}{(\bar{\rho})^n_{j+1/2}\Delta x_{j+1/2}}(p^n_{j+1} - p^n_j) + K^n_{j+1/2}(2\tilde{V}^{n+1}_{j+1/2} - V^n_{j+1/2})\,|V^n_{j+1/2}| = 0, \quad (7)$$

where

$$\beta = 0, \qquad \nabla_{j+1/2}\tilde{V}^n < 0$$
$$= 1, \qquad \nabla_{j+1/2}\tilde{V}^n > 0;$$

Basic Equations

$$(V^{n+1}_{j+1/2} - V^n_{j+1/2})/\Delta t + V^n_{j+1/2}\nabla_{j+1/2}\tilde{V}^{n+1} + \beta(V^{n+1}_{j+1/2} - V^n_{j+1/2})\nabla_{j+1/2}\tilde{V}^n + \frac{1}{(\bar{\rho})^n_{j+1/2}\Delta x_{j+1/2}}(\tilde{p}^{n+1}_{j+1} - \tilde{p}^{n+1}_j) + K^n_{j+1/2}(2V^{n+1}_{j+1/2} - V^n_{j+1/2})\,|V^n_{j+1/2}| = 0; \quad (8)$$

$$(\tilde{\rho}^{n+1}_j - \rho^n_j)/\Delta t + \nabla_j \cdot (\rho^n V^{n+1}) = 0; \quad (9)$$

$$(\tilde{\rho}^{n+1}_j \tilde{e}^{n+1}_j - \rho^n_j e^n_j)/\Delta t + \nabla_j \cdot (\rho^n e^n V^{n+1}) + \tilde{p}^{n+1}_j \nabla_j \cdot (V^{n+1}) = 0; \quad (10)$$

and

Stabilizer Mass and Energy Equations

$$(\rho^{n+1}_j - \rho^n_j)/\Delta t + \nabla_j \cdot (\rho^{n+1} V^{n+1}) = 0; \quad (11)$$

$$(\rho^{n+1}_j e^{n+1}_j - \rho^n_j e^n_j)/\Delta t + \nabla_j \cdot (\rho^{n+1} e^{n+1} V^{n+1}) + \tilde{p}^{n+1}_j \nabla_j \cdot (V^{n+1}) = 0. \quad (12)$$

A tilde above a variable indicates that it is the result of an intermediate step and not the final value for the time step. An overbar indicates a 50% average between its values at adjacent cells.

The material Courant stability limit is eliminated by treatment of the terms $V\nabla V$, $\nabla \cdot \rho V$, and $\nabla \cdot \rho e V$ during the two steps. These are the terms involved in the information propagation that was discussed in the Introduction. Additional robustness has been obtained with the peculiar form of the friction terms and the use of nonzero values of β in the $V\nabla V$ terms. These special terms for friction and $V\nabla V$ are obtained by linearizing similar terms that are fully implicit in velocity ($K^n_{j+1/2} V^{n+1}_{j+1/2}\,|V^{n+1}_{j+1/2}|$ and $V^{n+1}_{j+1/2}\nabla_{j+1/2}V^{n+1}$).

Equation (7) simply represents a tridiagonal linear system in the unknown $\tilde{V}^{n+1}$ and is solved first. Next, the coupled nonlinear system given by Eqs. (8)–(10) is solved. To accomplish this, Eq. (8) is rearranged to obtain V^{n+1} as a linear function of the new time pressures. This relation is substituted into Eqs. (9) and (10), along with thermodynamic relations that give density and energy as functions of pressure and temperature. The resulting pair of nonlinear vector equations is solved by Newton iteration for all new time pressures and temperatures. Simple algebraic manipulations can reduce the linear system that must be solved in this iteration to a tridiagonal system with the variation in $\tilde{p}^{n+1}$ as the unknown. Once these equations are solved, V^{n+1} is known and hence both Eqs. (11) and (12) are simple tridiagonal linear systems, with unknowns ρ_j^{n+1} and $\rho_j^{n+1}e_j^{n+1}$, respectively.

When this equation set is adapted to flow in complex piping networks, the pure tridiagonal structure is lost. The matrices, however, are still sparse and easily solved (see [3]).

The stability expected for these equations based on information flow arguments has been verified by a large number of computational test problems. When the friction factor (K) is a constant, we have not found any test problems that exhibit instabilities. At very large time steps, however, functional forms for the friction factor containing too much old time velocity dependence can drive instabilities. This is why the method is referred to as stability enhancing rather than unconditionally stable.

Because the basic form of the finite-difference operators (both spatial and temporal) is consistent between the two steps, the order of accuracy of the full SETS equations is the same (first order in space and time) as the basic semi-implicit equations (8)–(10). This consistency appears necessary to prevent the development of feedback oscillations between the two steps. It has the advantage of ensuring that, for small enough time steps, the results of any SETS calculation will approach those of the basic semi-implicit equations.

Some variations on this method are possible and perhaps even desirable for certain problems. For this specific pipe flow model, Eq. (7) can be eliminated and $\tilde{V}^{n+1}$ replaced by V^{n+1} in Eq. (8). With the proper solution procedure for Eqs. (8)–(10), this change will reduce computation costs. This variation, however, does not generalize well to multiphase flow equations with more than one equation of motion or to calculations in two or three dimensions, because the bandwidth of some matrices is increased. In some instances the more traditional ICE coupling of mass and motion equations could be used to replace Eqs. (8) and (9) and to eliminate Eq. (10) in favor of a temperature constraint, but the strong implicit coupling of the energy equation expressed by Eq. (10) is important in systems with reactions or phase change (see Liles and Reed [4]).

We have found the SETS method particularly valuable when applied to the two-fluid model of two-phase flow used in modeling nuclear reactor transients. For this model the stabilizer equations add less than 20% to the computational cost per cell per step of the basic equation set. A fully implicit method multiplies this cost by a factor of 6. The application of the method to these equations is described in [5–7]. Because these references are not widely available, the difference equations described

in [6] and [7] have been included in the Appendix. In these references an interesting variation on the finite-difference divergence operator was described that is superior in regions of rapid phase change to the one given here. The form of the $V\nabla V$ term also was different in [5], but the one given here in Eqs. (7) and (10) has proved to be superior.

III. Sample Calculation

The SETS method currently is available in TRAC–PF1, a best-estimate computer code for calculating loss-of-coolant accidents in nuclear reactors. TRAC–PF1 is described in detail in [6] and [7] and has been released to the National Energy Software Center at Argonne. The finite-difference equations used are a direct generalization of Eqs. (7)–(12) to the two-fluid model of two-phase flow and are identical to those equations in the limit of single-phase flow with no heat transfer. The sample calculation presented here uses this code to model a reactor accident similar to the one that occurred at Three Mile Island. During this hypothetical accident the reactor depressurized and voided due to flow through a pressure relief valve that jammed open.

The reactor system is represented with 80 spatial nodes. Throughout most of the system it is possible to use mesh lengths of a meter or more because of the small spatial gradients of all physical variables. In the pressure relief valve, however, these gradients are always large, and mesh lengths of a centimeter are required to model the choked flow accurately.

Figures 1 and 2 present the calculated pressure and fraction of water in the vapor

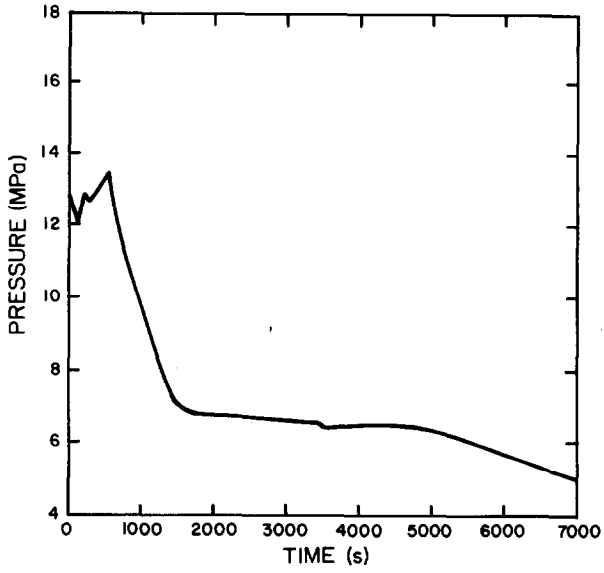

FIG. 1. System pressure vs time for a hypothetical nuclear reactor accident.

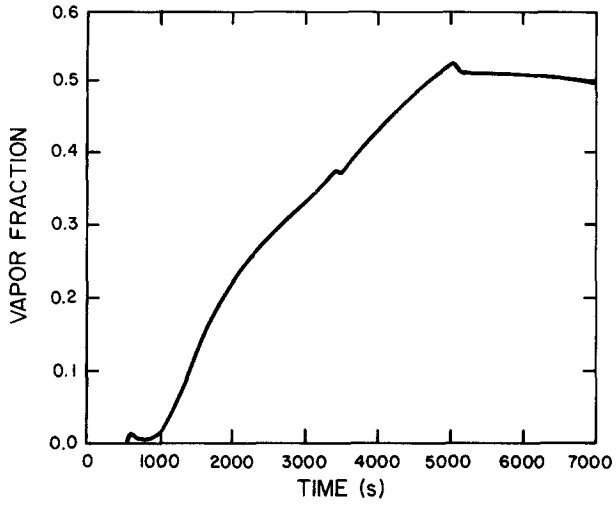

FIG. 2. Volume fraction occupied by steam near the top of the reactor core.

phase for a cell near the top of the reactor core. Unlike the actual incident at Three Mile Island, this accident scenario involved injection of enough coolant after 5000 s to prevent overheating of the nuclear rods. For our purpose, the most important feature of these results is the relatively slow rate of change of system conditions. This means that fairly large time-step sizes can be taken without affecting the accuracy of the calculations. During the base run of this problem, the time-step size was typically 3–6 s. Given the fluid velocities in the system for time steps in this range, the material Courant stability limit was exceeded by factors of 100,000 in the relief valve and by 10 to 20 in the main reactor loops, without producing numerical instabilities.

To check for errors induced by time-step size, a second run was made with the time steps forced to half the size of the preceding run. The curves corresponding to Figs. 1 and 2 overlaid the original results and the values matched closely for all other state variables in the system. This comparison indicates that errors due to time-step size were not significant and, hence, the results of the SETS code were very close to what would have been calculated by a semi-implicit code with the same spatial difference method. Similarly, good comparisons have been found for a number of simpler problems that were run both with SETS and with an equivalent semi-implicit code (see e.g., [5]).

No studies were made of errors due to spatial discretization because the SETS method was intended simply to improve stability of an existing finite-difference scheme without improving the order of accuracy. Possible adaptations of SETS to higher order methods will be studied in the future.

Because of the severe time-step restriction in the relief valve, no standard semi-implicit code could run efficiently on this problem with the spatial mesh that we used. Even if special treatment were given to the valve, such a code would be an order of magnitude slower than the SETS code due to the stability limit in the reactor loops.

IV. Conclusion

The SETS approach has proved to be a very flexible and efficient way to improve the stability of fluid flow calculations. The method is now beyond the demonstration phase and currently is being used for a wide range of nuclear reactor safety calculations. Most work thus far has been on adapting it to the one-dimensional two-phase flow equations used in modeling these reactor transients. However, work is under way at Los Alamos to adapt the method to a three-dimensional flow code. In the future this approach should prove extremely useful for diverse problems in combustion, multiphase, and reacting flow.

APPENDIX: SETS IN TRAC–PF1

The SETS method has been applied successfully to the modeling of two-phase flow in TRAC–PF1 [7]. In this code a three-component two-fluid model is described by seven differential equations.

Liquid Mass Equation

$$\frac{\partial(1-\alpha)\rho_l}{\partial t} + \nabla \cdot [(1-\alpha)\rho_l \mathbf{V}_l] = -\Gamma. \tag{A1}$$

Combined Vapor Mass Equation

$$\frac{\partial(\alpha\rho_g)}{\partial t} + \nabla \cdot (\alpha\rho_g \mathbf{V}_g) = \Gamma. \tag{A2}$$

Noncondensable Gas Mass Equation

$$\frac{\partial(\alpha\rho_a)}{\partial t} + \nabla \cdot (\alpha\rho_a \mathbf{V}_g) = 0. \tag{A3}$$

Combined Vapor Equation of Motion

$$\frac{\partial \mathbf{V}_g}{\partial t} + \mathbf{V}_g \cdot \nabla \mathbf{V}_g = -\frac{c_i}{\alpha\rho_g}(\mathbf{V}_g - \mathbf{V}_l)|\mathbf{V}_g - \mathbf{V}_l| - \frac{1}{\rho_g}\nabla p - \frac{c_{wg}}{\alpha\rho_g}\mathbf{V}_g|\mathbf{V}_g| + \mathbf{g}. \tag{A4}$$

Liquid Equation of Motion

$$\frac{\partial \mathbf{V}_l}{\partial t} + \mathbf{V}_l \cdot \nabla \mathbf{V}_l = \frac{c_i}{(1-\alpha)\rho_l}(\mathbf{V}_g - \mathbf{V}_l)|\mathbf{V}_g - \mathbf{V}_l| - \frac{1}{\rho_l}\nabla p - \frac{c_{wl}}{(1-\alpha)\rho_l}\mathbf{V}_l|\mathbf{V}_l| + \mathbf{g}. \tag{A5}$$

Combined Vapor Energy Equation

$$\frac{\partial}{\partial t}(\alpha\rho_g e_g) + \nabla \cdot (\alpha\rho_g e_g \mathbf{V}_g)$$

$$= -p\frac{\partial \alpha}{\partial t} - p\nabla \cdot (\alpha \mathbf{V}_g) + q_{wg} + q_{ig} + \Gamma h_{sg}. \tag{A6}$$

Total Energy Equation

$$\frac{\partial[(1-\alpha)\rho_l e_l + \alpha\rho_g e_g]}{\partial t} + \nabla \cdot [(1-\alpha)\rho_l e_l \mathbf{V}_l + \alpha\rho_g e_g \mathbf{V}_g]$$

$$= -p\nabla \cdot [(1-\alpha)\mathbf{V}_l + \alpha \mathbf{V}_g] + q_{wl} + q_{wg}. \tag{A7}$$

The subscript g denotes the combined vapor field and l, the liquid field. A subscript a is used for the noncondensable gas because that component generally is used to model air.

In these equations the microscopic vapor densities and energies are sums of the steam and noncondensable components

$$\rho_g = \rho_s + \rho_a \tag{A8}$$

and

$$\rho_g e_g = \rho_s e_s + \rho_a e_a. \tag{A9}$$

The average volume fraction of vapor (α) is used to obtain macroscopic densities and energies. We assume Dalton's law applies; therefore,

$$p = p_s + p_a. \tag{A10}$$

In addition to the thermodynamic relations that are required for closure, specifications for the interfacial drag coefficients (c_i), the interfacial heat transfer (q_{ig}), the phase-change rate (Γ), the wall shear coefficients (c_{wg} and c_{wl}), and the wall heat transfers (q_{wg} and q_{wl}) are required. Gamma is evaluated from a simple thermal energy jump relation,

$$\Gamma = \frac{-q_{ig} - q_{il}}{h_{sg} - h_{sl}}, \tag{A11}$$

where

$$q_{ig} = h_{ig} A_i \frac{(T_{ss} - T_g)}{\text{vol}} \tag{A12}$$

and

$$q_{il} = h_{il} A_i \frac{(T_{ss} - T_l)}{\text{vol}}. \tag{A13}$$

Here A_i and the h_i terms are the interfacial area and heat-transfer coefficients and T_{ss} is the saturation temperature corresponding to the partial steam pressure.

Wall heat-transfer terms assume the form

$$q_{wg} = h_{wg} A_{wg} \frac{(T_w - T_g)}{\text{vol}} \tag{A14}$$

and

$$q_{wl} = h_{wl} A_{wl} \frac{(T_w - T_l)}{\text{vol}}, \tag{A15}$$

where A_{wg} and A_{wl} are the actual heated surface areas of the cell.

When the SETS method is applied to this model, the first change from the simplified equations in Section II occurs in the definition of the finite-difference divergence operator (Eq. (5)). In TRAC–PF1 this operator is formulated to allow modeling of pipes with nonuniform cross-sectional areas:

$$\nabla_j \cdot (YV) = \frac{(A_{j+1/2}\langle YV\rangle_{j+1/2} - A_{j-1/2}\langle YV\rangle_{j-1/2})}{\text{vol}_j}, \tag{A16}$$

where A is the local cross-sectional area and vol_j is the volume of the jth cell.

The most significant change in SETS when it is adapted to a two-fluid model is the addition of predictor motion equations for the liquid and vapor:

$$\begin{aligned}
&\frac{(\hat{V}_g^{n+1} - V_g^n)}{\Delta t} + V_g^n \nabla_{j+1/2} \tilde{V}_g^n + \beta(\hat{V}_g^{n+1} - V_g^n) \nabla_{j+1/2} \tilde{V}_g^n \\
&\quad + \frac{c_i^n}{\overline{(\alpha\rho_g)}_{j+1/2}^n} [2(\hat{V}_g^{n+1} - \hat{V}_l^{n+1}) - (V_g^n - V_l^n)] \, |V_g^n - V_l^n| \\
&\quad + \frac{1}{\overline{(\rho_g)}_{j+1/2}^n} \frac{(p_{j+1}^n - p_j^n)}{\Delta X_{j+1/2}} + \frac{c_{wg}}{\overline{(\alpha\rho_g)}_{j+1/2}^n} (2\hat{V}_g^{n+1} - V_g^n) \, |V_g^n| + g \cos\theta = 0,
\end{aligned} \tag{A17}$$

where

$$\begin{aligned}
\beta &= 0, \quad \text{if} \quad \nabla_{j+1/2} V^n \leqslant 0; \\
&= 1, \quad \text{if} \quad \nabla_{j+1/2} V^n > 0.
\end{aligned}$$

$$\begin{aligned}
&\frac{(\hat{V}_l^{n+1} - V_l^n)}{\Delta t} + V_l^n \nabla_{j+1/2} \tilde{V}_l^n + \beta(\hat{V}_l^{n+1} - V_l^n) \nabla_{j+1/2} \tilde{V}_l^n \\
&\quad + \frac{c_i^n}{\overline{[(1-\alpha)\rho_l]}_{j+1/2}^n} [2(\hat{V}_l^{n+1} - \hat{V}_g^{n+1}) - (V_l^n - V_g^n)] \, |V_g^n - V_l^n| \\
&\quad + \frac{1}{\overline{(\rho_l)}_{j+1/2}^n} \frac{(p_{j+1}^n - p_j^n)}{\Delta X_{j+1/2}} \\
&\quad + \frac{c_{wl}}{\overline{[(1-\alpha)\rho_l]}_{j+1/2}^n} (2\hat{V}_l^{n+1} - V_l^n) \, |V_l^n| + g \cos\theta = 0.
\end{aligned} \tag{A18}$$

These two equations are used simply to provide a better interfacial drag force term in the stabilizer motion equations. When they are excluded, undamped numerical oscillations can occur.

The remaining difference equations are a straightforward generalization of Eqs. (7)–(12).

Stabilizer Equations of Motion

$$\frac{(\tilde{V}_g^{n+1} - V_g^n)}{\Delta t} + V_g^n \nabla_{j+1/2} \tilde{V}_g^{n+1} + \beta(\tilde{V}_g^{n+1} - V_g^n) \nabla_{j+1/2} \tilde{V}_g^n$$
$$+ \frac{c_i^n}{(\overline{\alpha\rho_g})_{j+1/2}^n} [2(\hat{V}_g^{n+1} - \hat{V}_l^{n+1}) - (V_g^n - V_l^n)] |V_g^n - V_l^n|$$
$$+ \frac{1}{(\overline{\rho_g})_{j+1/2}^n} \frac{(p_{j+1}^n - p_j^n)}{\Delta X_{j+1/2}} + \frac{c_{wg}}{(\overline{\alpha\rho_g})_{j+1/2}^n} (2\tilde{V}_g^{n+1} - V_g^n) |V_g^n| + g \cos\theta = 0. \tag{A19}$$

$$\frac{(\tilde{V}_l^{n+1} - V_l^n)}{\Delta t} + V_l^n \nabla_{j+1/2} \tilde{V}_l^{n+1} + \beta(\tilde{V}_l^{n+1} - V_l^n) \nabla_{j+1/2} \tilde{V}_l^n$$
$$+ \frac{c_i^n}{[\overline{(1-\alpha)\rho_l}]_{j+1/2}^n} [2(\hat{V}_l^{n+1} - \hat{V}_g^{n+1}) - (V_l^n - V_g^n)] |V_g^n - V_l^n|$$
$$+ \frac{1}{(\overline{\rho_l})_{j+1/2}^n} \frac{(p_{j+1}^n - p_j^n)}{\Delta X_{j+1/2}}$$
$$+ \frac{c_{wl}}{[\overline{(1-\alpha)\rho_l}]_{j+1/2}^n} (2\tilde{V}_l^{n+1} - V_l^n) |V_l^n| + g \cos\theta = 0. \tag{A20}$$

Basic Equations of Motion

$$\frac{(V_g^{n+1} - V_g^n)}{\Delta t} + V_g^n \nabla_{j+1/2} \tilde{V}_g^{n+1} + \beta(V_g^{n+1} - V_g^n) \nabla_{j+1/2} \tilde{V}_g^n$$
$$+ \frac{c_i^n}{(\overline{\alpha\rho_g})_{j+1/2}^n} [2(V_g^{n+1} - V_l^{n+1}) - (V_g^n - V_l^n)] |V_g^n - V_l^n|$$
$$+ \frac{1}{(\overline{\rho_g})_{j+1/2}^n} \frac{(\tilde{p}_{j+1}^{n+1} - \tilde{p}_j^{n+1})}{\Delta X_{j+1/2}} + \frac{c_{wg}}{(\overline{\alpha\rho_g})_{j+1/2}^n} (2V_g^{n+1} - V_g^n) |V_g^n| + g \cos\theta = 0. \tag{A21}$$

$$\frac{(V_l^{n+1} - V_l^n)}{\Delta t} + V_l^n \nabla_{j+1/2} \tilde{V}_l^{n+1} + \beta(V_l^{n+1} - V_l^n) \nabla_{j+1/2} \tilde{V}_l^n$$
$$+ \frac{c_i^n}{[\overline{(1-\alpha)\rho_l}]_{j+1/2}^n} [2(V_l^{n+1} - V_g^{n+1}) - (V_l^n - V_g^n)] |V_l^n - V_g^n|$$

$$+\frac{1}{(\bar{\rho}_l)^n_{j+1/2}}\frac{(\tilde{p}^{n+1}_{j+1}-\tilde{p}^{n+1}_j)}{\Delta X_{j+1/2}}$$

$$+\frac{c_{wl}}{[(1-\alpha)\rho_l]^n_{j+1/2}}(2V^{n+1}_l - V^n_l)\,|V^n_l| + g\cos\theta = 0. \tag{A22}$$

Basic Mass Equations

$$\frac{[(\tilde{\alpha}\tilde{\rho}_g]^{n+1}-(\alpha\rho_g)^n]}{\Delta t} + \nabla_j\cdot(\alpha\rho_g V^{n+1}_g) = \tilde{\Gamma}^{n+1}. \tag{A23}$$

$$\frac{[(\tilde{\alpha}\tilde{\rho}_a)^{n+1}-(\alpha\rho_a)^n]}{\Delta t} + \nabla_j\cdot(\alpha\rho_a V^{n+1}_g) = 0. \tag{A24}$$

$$\frac{[(1-\tilde{\alpha})^{n+1}\tilde{\rho}^{n+1}_l-(1-\alpha)^n\rho^n_l]}{\Delta t} + \nabla_j\cdot[(1-\alpha)\rho_l V^{n+1}_l] = -\tilde{\Gamma}^{n+1}. \tag{A25}$$

Basic Energy Equations

$$\frac{[(\tilde{\alpha}\tilde{\rho}_g\tilde{e}_g)^{n+1}-(\alpha\rho_g e_g)^n]}{\Delta t} + \nabla_j\cdot(\alpha\rho_g e_g V^{n+1}_g)$$

$$+\tilde{p}^{n+1}\left[\frac{(\tilde{\alpha}^{n+1}-\alpha^n)}{\Delta t} + \nabla_j\cdot(\alpha^n V^{n+1}_g)\right] = \tilde{q}^{n+1}_{wg} + \tilde{q}^{n+1}_{ig} + \tilde{\Gamma}^{n+1}\tilde{h}^{n+1}_{sg}. \tag{A26}$$

$$\frac{\{[\tilde{\alpha}\tilde{\rho}_g\tilde{e}_g + (1-\tilde{\alpha})\tilde{\rho}_l\tilde{e}_l]^{n+1} - [\alpha\rho_g e_g + (1-\alpha)\rho_l e_l]^n\}}{\Delta t}$$

$$+\nabla_j\cdot[(\alpha\rho_g e_g)V^{n+1}_g + (1-\alpha)\rho_l e_l V^{n+1}_l]$$

$$+\tilde{p}^{n+1}\nabla_j\cdot[(1-\alpha)^n V^{n+1}_l + \alpha^n V^{n+1}_g] = \tilde{q}^{n+1}_{wg} + \tilde{q}^{n+1}_{wl}. \tag{A27}$$

Stabilizing Mass Equations

$$\frac{[(\alpha\rho_g)^{n+1}-(\alpha\rho_g)^n]}{\Delta t} + \nabla_j\cdot[(\alpha\rho_g)^{n+1}V^{n+1}_g] = \tilde{\Gamma}^{n+1}. \tag{A28}$$

$$\frac{[(\alpha\rho_a)^{n+1}-(\alpha\rho_a)^n]}{\Delta t} + \nabla_j\cdot[(\alpha\rho_a)^{n+1}V^{n+1}_g] = 0. \tag{A29}$$

$$\frac{[(1-\alpha)^{n+1}\rho^{n+1}_l-(1-\alpha)^n\rho^n_l]}{\Delta t} + \nabla_j\cdot[(1-\alpha)^{n+1}\rho^{n+1}_l V^{n+1}_l] = -\tilde{\Gamma}^{n+1}. \tag{A30}$$

Stabilizing Energy Equations

$$\frac{[(\alpha\rho_g e_g)^{n+1} - (\alpha\rho_g e_g)^n]}{\Delta t} + \nabla_j \cdot [(\alpha\rho_g e_g)^{n+1} V_g^{n+1}]$$

$$+ \tilde{p}^{n+1} \left[\frac{(\tilde{\alpha}^{n+1} - \alpha^n)}{\Delta t} + \nabla_j \cdot (\alpha^n V_g^{n+1})\right] = \tilde{q}_{ig}^{n+1} + \tilde{q}_{wg}^{n+1} + \tilde{\Gamma}^{n+1}\tilde{h}_{sg}^{n+1}. \quad \text{(A31)}$$

$$\frac{\{[(1-\alpha)\rho_l e_l]^{n+1} - [(1-\alpha)\rho_l e_l]^n\}}{\Delta t} + \nabla_j \cdot \{[(1-\alpha)\rho_l e_l]^{n+1} V_l^{n+1}\}$$

$$+ \tilde{p}^{n+1} \left\{\frac{(\alpha^n - \tilde{\alpha}^{n+1})}{\Delta t} + \nabla_j \cdot [(1-\alpha)^n V_l^{n+1}]\right\} = \tilde{q}_{wl}^{n+1} - \tilde{q}_{ig}^{n+1} - \tilde{\Gamma}^{n+1}\tilde{h}_{sg}^{n+1}. \quad \text{(A32)}$$

A caret above velocities denotes explicit predictor values. If there are no subscripts denoting cell location, we assume subscript j for mass and energy equations and subscript $j + \frac{1}{2}$ for equations of motion. Finally, theta is the angle between a vector from the center of cell j to the center of cell $j + 1$ and a vector against gravity.

Time levels were omitted from some flux terms in Eqs. (38)–(42) because these terms contain both old and new time quantities. If X is a combination of state variables without a time superscript, then the correct definition for the divergence term in which it appears is

$$\nabla_j(XV_j^{n+1}) = \{A_{j+1/2} V_{j+1/2}^{n+1}[f_{j+1/2} X_j^m + (1 - f_{j+1/2}) X_{j+1}^n]$$
$$- A_{j-1/2} V_{j-1/2}^{n+1}[f_{j-1/2} X_{j-1}^n + (1 - f_{j-1/2}) X_j^m]\}/\text{vol}_j, \quad \text{(A33)}$$

where

$$X_j^m = g' X^n + (1 - g') X_j^{n+1}. \quad \text{(A34)}$$

The weighting function used to obtain donor-cell averaging (Eq. (4)) is f and g' is a weighting factor that depends on the rate of phase change, which goes to unity as the phase change disappears and to zero as the phase change approaches the total outflow of the phase created in the cell. For nonzero g', this form of the divergence operator is nonconservative but total conservation is maintained by the stabilizer step.

The solution of the finite-difference equations is a direct generalization of the method described for the simplified equations. There is no coupling between stabilizer equations for different fields, so each is solved exactly like its counterpart in Section II. The reduced form of the basic equation set is combined with the appropriate thermodynamic relations and solved for the unknowns $\tilde{p}^{n+1}$, $\tilde{p}_a^{n+1}$, $\tilde{T}_g^{n+1}$, $\tilde{T}_l^{n+1}$, and $\tilde{\alpha}^{n+1}$.

ACKNOWLEDGMENT

This work was sponsored by the United States Nuclear Regulatory Commission.

REFERENCES

1. F. H. HARLOW AND A. A. AMSDEN, *J. Comput. Phys.* **8** (1971), 197.
2. J. DOUGLAS AND H. H. RACHFORD, *Trans. Amer. Math. Soc.* **82** (1956), 421.
3. "TRAC–PD2: An Advanced Best-Estimate Computer Program for Pressurized Water Reactor Loss-of-Coolant Accident Analysis," Los Alamos National Lab. Rep. LA–8709–MS, NUREG/CR–2054 (1981).
4. D. R. LILES AND W. H. REED, *J. Comput. Phys.* **26** (1978), 390.
5. J. H. MAHAFFY, "A Stability Enhancing Two-Step Method for One-Dimensional Two-Phase Flow," Los Alamos Scientific Lab. Rep. LA–7951–MS, NUREG/CR–0971 (1979).
6. J. H. MAHAFFY, D. R. LILES, AND T. F. BOTT, TRAC Methods and Models, "Proceedings, American Nuclear Society Specialists Meeting on Small Break Loss-of-Coolant Accident Analyses in LWRs," Electric Power Research Inst. Rep. WS–81–201 (1981).
7. "TRAC–PF1: A Fast Running Advanced Best-Estimate Computer Program for PWR LOCA Analysis," Los Alamos National Lab. Rep., to be published.